JOURNAL OF APPLIED ELECTROCHEMISTRY **22** (1992) 959–965

Correlation between the electrochemical properties of colloidal oxides and supported oxides on metallic substrates

M. J. AVENA, R. CABROL, O. R. CÁMARA*, C. P. DE PAULI

Departamento de Físico Química, Facultad de Ciencias Químicas, Universidad Nacional de Córdoba. Suc. 16, C.C. 61, 5016 Córdoba, Argentina

Received 11 December 1990; revised 12 April 1991

Mixed oxide electrodes of Ti(IV) and Cr(III) were prepared by calcining $Cr(OH)_3$ layers deposited on metallic titanium supports. This treatment produced a mixed oxide film of TiO_2–Cr_2O_3 covered with a layer of pure Cr_2O_3. The electrochemical response (cyclic voltammetry) shows the presence of two or three oxidation peaks depending on the electrode preparation conditions. One peak may be interpreted as the oxidation of Cr(III) to Cr(VI) species and the appearance of other peaks is due to the presence of chromium atoms in oxidation states higher than (III). The results of chemical analyses, electrophoretic mobilities and acid-base potentiometric titrations on calcined $Cr(OH)_3$ powders shows that the calcination step in air produced the decomposition of the Cr(III) hydroxide to the Cr(VI) oxide. Soluble Cr(VI) compounds were found in equilibrium with the suspended powder oxide which markedly affected the shape of the titrations curves. From the amount of Cr(VI) present in solution it was possible to correct the experimental σ_0-pH curves. These corrected data indicated that Cr(VI) soluble species adsorbed at the Cr_2O_3/electrolyte interface.

1. Introduction

The study of colloidal phenomena in metal oxides suspended in aqueous media has gone beyond academic interest because many technological processes involving oxide materials are, to some extent, controlled by the structure and characteristics of the oxide/aqueous solution interface [1]. The amphoteric characteristic of the metallic oxide surface is given by the acid-base properties of the surface hydroxyl groups and several mathematical models of the oxide/electrolyte electric double layer have been developed from these properties [1]. A clear understanding of these surface phenomena is not only necessary for the development of the chemistry of colloids but also for a better interpretation of the electrochemical processes taking place in the oxide electrode/solution interface.

With regard to electrodes formed by oxide materials, most of the systems that have been prepared and studied had a metallic titanium substrate as a supporting conductor and an oxide surface layer of one or more metal ions, generally transition elements. These electrodes have commonly been named Dimensionally Stable Anodes (DSA®) due to their stability in industrial chlor-alkali processes. Their application as anodes for organic electrosynthesis has received some attention, where Ti/TiO_2–Cr_2O_3 electrodes have been used to oxidize different alcohols [2–5]. The most common method for preparing these electrodes has been coating the substrate with a solution of chloride-metal salt dissolved in a non-aqueous solvent and then firing it at moderately high temperature.

In this laboratory the Ti(IV) and Cr(III) mixed oxide electrodes were prepared by calcination at different temperatures of a chromium(III) hydroxide precursor deposited on a titanium substrate [6–8].

The present work is concerned with the surface characteristics of Ti/TiO_2–Cr_2O_3 electrodes [9] both by means of techniques commonly used in colloidal systems of oxide powder materials together with electrochemical methods currently applied in electrolytic cells.

2. Experimental details

2.1. *Ti/TiO_2–Cr_2O_3 electrodes*

2.1.1. Materials. The Ti(IV) and Cr(III) mixed oxide electrodes were prepared by coating a foil of titanium metal with a measured volume of an aqueous suspension of chromium(III) hydroxide. This suspension was prepared by alkaline precipitation of a 0.1 M $CrK(SO_4)_2$ solution using a 1 M NaOH solution added dropwise until a pH of 9.0 was reached (the minimum solubility pH of $Cr(OH)_3$). The precipitate was centrifuged and the supernatant removed, deionized water was added and the solid was redispersed by ultrasonic stirring. This treatment was repeated several times. Finally, the washed solid was re-suspended and the

---

* To whom all correspondence should be addressed.

0021-891X/92

final volume was adjusted in order to achieve a 0.1 M concentration of $Cr(OH)_3$.

The metallic substrates were titanium sheets or discs (Koch-Light 99.98%) 0.8–1.0 cm^2 in area, pretreated with a chemical polishing by immersion in an ultrasonically stirred mixture of HF (48%) : HNO_3 (65%) : H_2O with a 1 : 4 : 5 volume ratio for 15 s, then mechanically polished using 600 and 1200 grade CSi paper and finally ultrasonically degreased in acetone.

In order to obtain the $Ti/TiO_2–Cr_2O_3$ electrodes, the desired volume of the hydroxide suspension was poured onto the clean substrate with a microsyringe, completely spread, dried in a current of hot air and then calcined at different temperatures between 350 and 750° C in an atmosphere of air. This treatment consisted of increasing the temperature to a predetermined value at a rate of $10° C\,min^{-1}$ and then holding at this value for different times. Under these conditions dehydration of the deposited $Cr(OH)_3$ was produced together with thermal oxidation of the titanium substrate. This treatment produced a surface film of $TiO_2–Cr_2O_3$ mixed oxide covered with some pure Cr_2O_3 on the metallic titanium [8].

2.1.2. *Electrochemical experiences.* The electronic equipment used to obtain the potentiodynamic *i–E* profiles of these electrodes in the electrochemical experiments was a LyP potentiostat, an EG&G Parc 175 wave generator and an X–Y Omnigraphic 2000 Houston Instrument recorder. The potential sweep rate in all the experiments was $0.1\,V\,s^{-1}$ applied initially in the anodic sense from the measured rest potential. The counter-electrode was a large area platinum foil and the reference electrode was a saturated calomel electrode (SCE) to which all potential values are referred.

2.2. *Preparation of powder materials*

2.2.1. *Synthesis of $Cr(OH)_3$ powders.* Chromium(III) hydroxide powder samples were synthesized by adding 300 mL of a 1.1 M NaOH solution dropwise to 1 dm^3 of 0.11 M $CrK(SO_4)_2$ solution at a rate of one drop per second. The resulting suspension was heated at 85° C for 48 h with continuous stirring in a reflux system and later centrifuged and filtered. The solid material thus obtained was washed several times with deionized water until a constant conductivity of the supernatant was reached. The pH value of the supernatant after the last stage of washing was 7.5. The chromium(III) hydroxide solid sample finally obtained was dried at 110° C for 48 h in an air atmosphere to remove adsorbed water.

2.2.2. *Synthesis of Cr_2O_3 powders.* Different powder samples of chromium(III) oxide were synthesized from the chromium(III) hydroxide samples obtained previously by calcination at 400, 500 and 600° C for 2 h in an air atmosphere.

2.2.3. *X-ray diffraction analyses.* X-ray diffractograms of the chromium(III) hydroxide and oxide samples were obtained with a Philips PW 1140 diffractometer using the Ni filtered CuK_α emission line. The powdered samples were placed on glass supports, oriented and rotated at a rate of $2\theta\,min^{-1}$, recording the diffractogram for 2θ between 12° and 60°.

2.3. *Surface characterization of the powder materials*

2.3.1. *Measurement of surface areas.* The specific surface area of the different powder samples of chromium(III) oxide was determined by nitrogen adsorption, considering a $16.2 \times 10^{-20}\,m^2$ area per adsorbed nitrogen molecule.

2.3.2. *Electrophoretic mobilities.* The electrophoretic mobilities of chromium(III) hydroxide and oxide samples were measured using Mark II Rank Brothers microelectrophoresis equipment in order to determine their isoelectric point values (IEP). A pH range of 3.0 to 10.0 was selected to avoid effects of chemical dissolution of the samples. The IEP is the pH value for which the electrophoretic mobility of the particle is zero and corresponds to a situation where the net charge in the slipping plane of the suspended colloidal particles is zero. In practice, this plane is considered to be located on the plane from which the diffuse layer in the particle/solution interface is formed.

For these experiments a certain amount of the sample was suspended in a 0.01 M KCl solution and ultrasonically dispersed. The resulting suspensions were allowed to reach equilibrium at a given pH achieved by adding different amounts of HCl or KOH solutions. The values of the electrophoretic mobilities were taken at each pH value as an average of about ten pairs of readings which were carried out by alternating the polarity of the electrodes.

2.3.3. *Acid-base potentiometric titrations.* This method is generally used for the determination of the surface charge (σ_0) of suspended particles of clays, metallic oxides and other compounds [10]. Therefore, 0.5–0.7 g samples of chromium(III) oxide were suspended by ultrasonic stirring in $NaNO_3$ 0.001 to 0.5 M solutions and were allowed to reach equilibrium under continuous stirring conditions and degassed for the required time. The pH value thus obtained was marked the zero point of titration (ZPT) and from this point small volumes of standard solutions of HNO_3 or NaOH were added. The pH value after each addition was recorded when its variation was lower than $0.1\,mV\,min^{-1}$. In these experiments an ORION BN 9109 glass pH electrode, a double-junction Ag/AgCl/Cl^- ORION 900200 electrode as reference and an automatic ORION 960 titration equipment were used. The pH values obtained under equilibrium conditions were plotted as a function of σ_0. This parameter was calculated as ($\Gamma_{H^+} - \Gamma_{OH^-}$), that is, as the difference

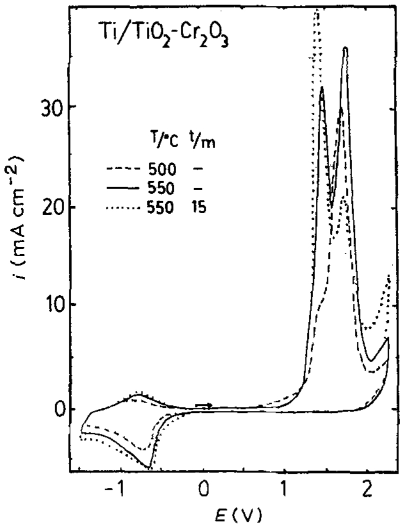

Fig. 1. Potentiodynamic *i–E* profiles for Ti/TiO_2–Cr_2O_3 electrodes obtained at different calcination temperatures and times. Electrolyte 0.5 M Na_2SO_4 at pH 9.0. Potential sweep rate: 0.1 V s^{-1}.

between the total H^+ or OH^- ions added to the suspension and those required to carry out a titration of a blank solution of the same saline concentration to the same pH value. On the other hand, the zero value of the charge axis for the potentiometric acid-base titrations at each ionic strength is fixed at the intersection point between the oxide sample titration and the corresponding blank titration curves.

According to the most common models of the electric double layer [11–13] and considering the absence of specific adsorption from the electrolyte [14], the common intersection point of the titration curves (CIP) at different ionic strengths is the pH value of zero charge (or zero point of charge, ZPC) of the suspended oxide, i.e., the pH solution at which the net charge on the surface plane of the particle is zero.

3. Results and discussion

3.1. *Voltammetric analyses*

The electrochemical response of the Ti/TiO_2–Cr_2O_3 electrodes prepared by calcination of a coating of aqueous suspension of chromium(III) hydroxide over titanium substrates to produce a thin mixed oxide layer gives rise to a complex anodic process starting up at about 1.1 V/SCE showing the presence of mainly two (eventually three) current peaks, depending on the electrode preparation conditions. In Fig. 1 several voltamperograms obtained in 0.5 M Na_2SO_4 solution at pH 9.0 using electrodes prepared with slightly different calcination temperatures and times are shown. The effect of lower or higher temperatures than those indicated in the figure and more prolonged times than several minutes in the calcination step produce more drastic changes in the voltamperometric curve [15].

Some general characteristics of the potentiodynamic behaviour of these Ti(IV) and Cr(III) mixed oxide electrodes have been previously reported [8], particularly for substrates initially coated with a gel layer of pure chromium(III) hydroxide and/or a mixed gel of Ti(IV) and Cr(III) hydroxides in a Cr/Ti mol ratio of 75 : 25. These electrodes showed only one anodic process around 1.62 V with a maximum current value for calcination temperatures between 500 and 550° C. This process was interpreted in terms of the oxidation reaction in a slightly basic solution

$$Cr_2O_3(s) + 10\,OH^- \longrightarrow 2\,CrO_4^{2-}(aq) + 5\,H_2O + 6e^- \qquad (1)$$

in a similar way to those proposed by other authors [3, 4] for a highly acidic media.

The more complex response in the anodic potential range reported here may be interpreted in terms of the presence of some chromium oxide species in the surface layer having a higher oxidation state than Cr(III) which are formed due to a decomposition reaction from chromium(III) hydroxide species during the calcination in air.

The role of the hydroxide species in producing a decomposition reaction to higher oxidation states has been found by Hill *et al.* [16] by performing experiments of temperature programmed reduction/oxidation (TPR/O) on silica-supported chromic acid catalyst. They observed a TPO peak at 830 K corresponding to a particle surface level oxidation from Cr(III) to Cr(VI) species due to molecular oxygen, with the first chromium species having hydroxyl groups in their structure.

The results presented here, and the importance of the calcination environment, have been corroborated by other results obtained with electrodes whose calcination step was made in a controlled atmosphere. The effect of the different gaseous compositions during this stage drastically affects the appearance and the relationship in maximum current between the anodic current peaks [15].

The current-potential response obtained with these electrodes does not significantly change when the pH of the working solution is adjusted to different pH values between 2.0 and 12.5 (Fig. 2). The peak potentials remain practically constant (Fig. 3) though the charge of the whole anodic process increases slightly for more alkaline pH values (Fig. 4). This is, in principle, a surprising result since all the reactions involving the oxidation of chromium oxide species to higher oxidation states involve H^+ (or OH^-) ions and the dependence of the potentials with pH is well known [17, 18]. For example,

$$Cr_2O_3 + H_2O \Longleftrightarrow 2CrO_2 + 2H^+ + 2e^-$$

$$E = 0.82 - 0.059\mathrm{pH} \qquad (2)$$

$$CrO_2 + H_2O \Longleftrightarrow CrO_3 + 2H^+ + 2e^-$$

$$E = 1.19 - 0.059\mathrm{pH} \qquad (3)$$

$$Cr_2O_3 + 5H_2O \Longleftrightarrow 2CrO_4^{2-} + 10H^+ + 6e^-$$

$$E = 0.94 - 0.098\mathrm{pH} \qquad (4)$$

In consequence, for these electrodes the anodic electro-oxidation process does not depend on the bulk

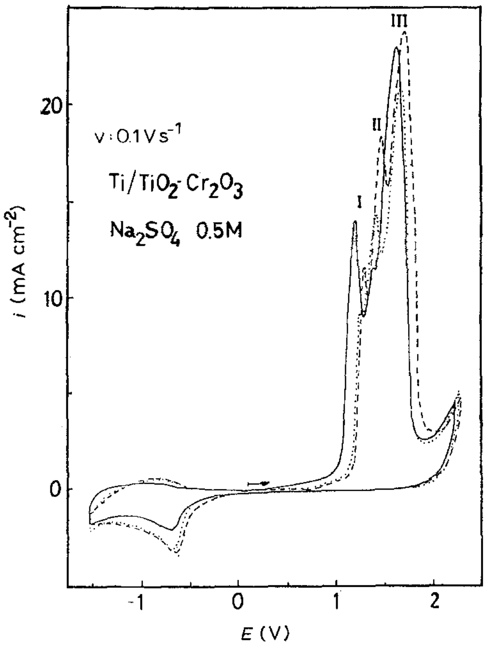

Fig. 2. Potentiodynamic i–E profiles for three different solution pH values: (· · · ·) 3.45; (– – – –) 7.75; (——) 11.00. Electrodes calcined up to 550°C where the temperature was held for 5 min.

pH, at least in the way predicted from thermodynamic considerations, suggesting that the electron transfer process occurs in an inner region of the surface mixed oxide layer.

Experiments recording the rest potential of these electrodes (measured at open circuit) as a function of electrolyte pH showed a linear variation with a slope of -34 and -46 mV per pH unit for 0.05 and 0.5 M Na_2SO_4, respectively (Fig. 5). This response in the rest potential to the change in pH indicates the existence of a relation between the electrode potential and the development and changes of the surface charge of the oxide layer as a consequence of the acid-base dissociation equilibria of the surface hydroxyl groups of the chromium oxide with the concentration of H^+ (or OH^-) ions in the bulk solution. These equilibria are

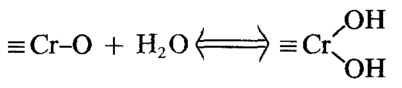
$$\equiv Cr\text{-}O + H_2O \rightleftharpoons \equiv Cr\begin{smallmatrix}OH\\ OH\end{smallmatrix} \quad (5)$$

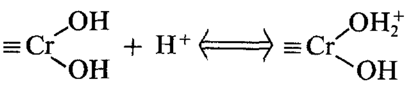
$$\equiv Cr\begin{smallmatrix}OH\\ OH\end{smallmatrix} + H^+ \rightleftharpoons \equiv Cr\begin{smallmatrix}OH_2^+\\ OH\end{smallmatrix} \quad (6)$$

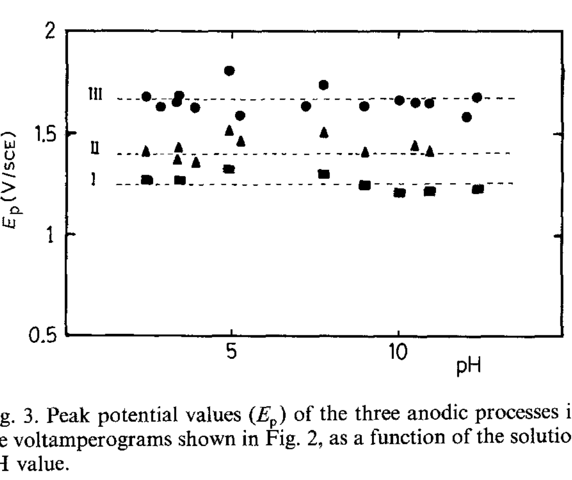

Fig. 3. Peak potential values (E_p) of the three anodic processes in the voltamperograms shown in Fig. 2, as a function of the solution pH value.

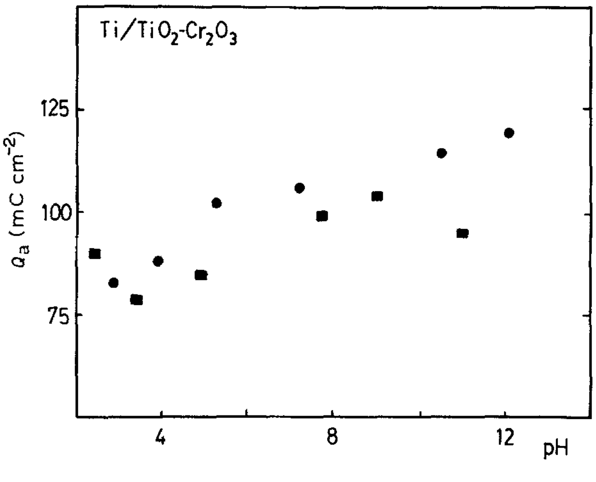

Fig. 4. Charge for the complete anodic process (Q_a) corresponding to the voltamperograms shown in Fig. 2. Two different sets of experiments.

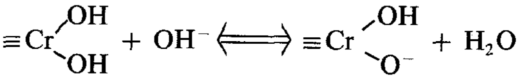
$$\equiv Cr\begin{smallmatrix}OH\\ OH\end{smallmatrix} + OH^- \rightleftharpoons \equiv Cr\begin{smallmatrix}OH\\ O^-\end{smallmatrix} + H_2O \quad (7)$$

with Equation 5 corresponding to the initial step of dissociative adsorption of water molecules on the dehydrated oxide surface to produce two hydroxyl groups having unequal acid-base properties, Equations 6 and 7.

Through a thermodynamic analysis of the adsorption/desorption process of H^+ ions on oxide surfaces, it is possible to predict [13] a dependence of $0.059\,V\,pH^{-1}$ between the oxide surface potential (relative to that in the bulk solution) and the H^+ ion concentration in solution, whenever the equilibrium constants corresponding to Equations 6 and 7 are large and similar. On the other hand, Ardizzone *et al.* [19] have found lower values for this dependence

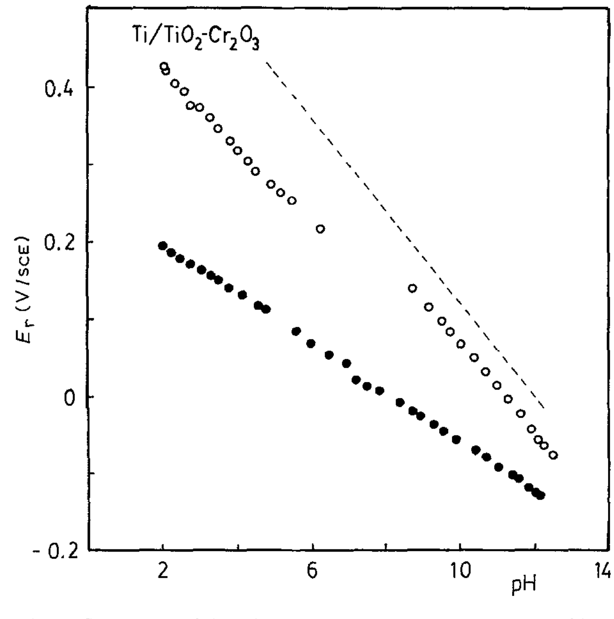

Fig. 5. Rest potential (E_r) values (measured at open circuit) of Ti/TiO_2–Cr_2O_3 electrodes, as a function of the solution pH value, for two different electrolyte concentrations. Calcination treatments of the electrodes were similar to those reported for Fig. 2. The dotted line corresponds to a slope of $0.059\,V\,pH^{-1}$. Na_2SO_4 concentration: (○) 0.5 and (●) 0.05 M.

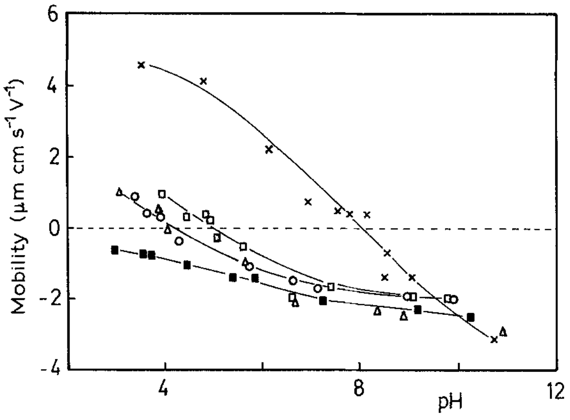

Fig. 6. Electrophoretic mobilities for chromium(III) hydroxide calcined at different temperatures, as a function of the solution pH value. Electrolyte (×, △, □, ○ at 110, 400, 500 and 600° C, respectively) 0.01 M KCl and (■) 0.01 M Na_2SO_4 at 500° C.

with zirconium dioxide. This occurs when the space charge density in the oxide phase provides a determining step in the fast establishment of an electroneutrality equilibrium in charge along the system support/mixed oxide layer/solution or when the surface charge density is small enough. However, it is clearly observed that the surface potential of the electrode responds to the solution pH while the peak potentials of the anodic electro-oxidation processes do not. This supports the conclusion that the electron transfer process must be occurring in an inner layer of the mixed oxide surface film.

3.2. *Surface characteristics of powder materials*

To clarify the surface behaviour of chromium oxides, several studies were carried out on powder samples of the precursor material used in the electrode coating.

The loss of mass by dehydration observed in the calcination of the $Cr(OH)_3$ powder samples at different temperatures was 25.9, 26.7 and 26.9% at 400, 500 and 600° C, respectively. These values are in good agreement with those corresponding to the reaction

$$2Cr(OH)_3(s) \longrightarrow Cr_2O_3(s) + 3H_2O(v) \qquad (8)$$

whose theoretical mass loss is 26.2%, and agrees with thermo-gravimetric analyses obtained with pure $Cr(OH)_3$ [8].

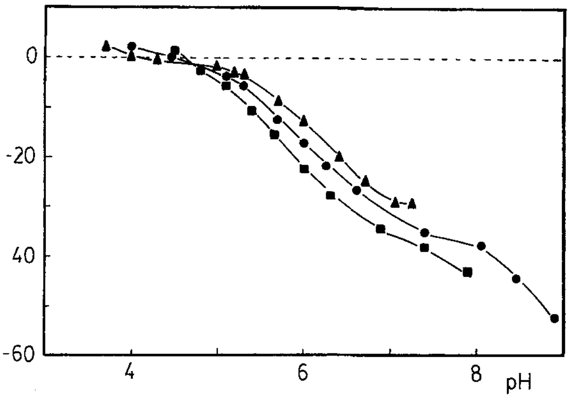

Fig. 7. Potentiometric titration curves for a chromium(III) oxide sample obtained from calcination to 500° C. $NaNO_3$: (■) 0.5, (●) 0.1 and (▲) 0.05 N.

The X-ray diffraction analyses showed that the samples of $Cr(OH)_3$ dried at 110° C are amorphous whereas those samples calcined at different temperatures from 400° C showed a crystalline structure with the same diffraction pattern. The main lines of the diffractogram coincide with the values reported in the literature [20, 21] for α-Cr_2O_3 and are shown in Table 1.

The determinations of the specific surface areas did not show significant differences except for the chromium oxide samples obtained at the highest temperature; their values being 34, 30, 32 and 20 $m^2\,g^{-1}$ for $Cr(OH)_3$ and Cr_2O_3 prepared at 400, 500 and 600° C, respectively. The lower value obtained for the 600° C sample may be attributed to the sintering effects of the crystallites.

The Cr(III) hydroxide sample showed an IEP of about 8.0 in 0.01 M KCl solution (Fig. 6) whereas those of the Cr(III) oxide samples were between 4.0 and 5.0. No significant differences were observed due to the different temperatures used in their preparation. In contrast, the samples of Cr(III) oxide calcined at 500° C and suspended in a 0.01 M Na_2SO_4 solution showed negative electrophoretic mobilities even at pH's lower than 3.0, indicating that a considerable adsorption of sulphate ions is taking place in the surface of the colloidal particles in this medium.

The CIP values obtained from the acid-base potentiometric titrations for the different calcined samples are in good agreement with the IEP obtained from electrophoretic measurements. In Fig. 7 the titration curves at different ionic strengths for Cr_2O_3 obtained at 500° C are shown. The corresponding behaviour of the other oxide samples does not differ significantly. Some preliminary experimental results showed no significant differences between KCl and $NaNO_3$ electrolytes.

However, the shape of the titration curves does not agree with those predicted for the different models [13, 22]. According to these models, the adsorption of H^+ and OH^- ions on the surface of an oxide increases exponentially from the zero point of charge towards lower and higher pH values, respectively. Therefore, an inflection point should be observed at the value of the ZPC where the buffer capacity of the system is lower. In all the titration curves two inflection points at pH 4.0–4.5 and at 7.5–8.0 were observed. On the other hand, a good correlation of the experimental data of the surface charge-pH with the theoretical curves from the triple layer model [11] can be obtained only if, for the latter, a capacity value for the region between the plane of surface charge (the surface of the solid particle) and the β plane (the inner Helmholtz

Table 1. Main emission lines by X-ray diffraction (2θ/deg)

Experimental	24.5	33.5	36.5	41.5	50.5	55.0
Reference [20]	24.65	34.05	36.43	41.6	50.49	55.35

plane) of around 700 μF cm^{-2} is considered. It should be pointed out here that the capacity values necessary to obtain a good fitting of the experimental results are dependent on the model to be used for describing the oxide/aqueous solution interface. For instance, the models based on a simple interface structure of Gouy-Stern type [23] require higher capacity values (400–500 μF cm^{-2}) to reproduce the experimental data theoretically, whereas for other more complex models, such as the triple layer model, values between 50 and 200 μF cm^{-2}, [22], are required.

A capacity value as high as 700 μF cm^{-2} implies that the thickness of the region between the surface and the β planes is much thinner than that reported in the literature [22] and even smaller than the ionic radius of the adsorbed cations.

On the other hand, the surface charge values shown in Fig. 7 are largely higher than those obtained by Yates and Healy for α-Cr_2O_3 [24] and by other authors [22] for different oxide samples. The former measured the development of the surface charge in α-Cr_2O_3 through salt titration with KNO_3 and obtained values around 5 μC cm^{-2} for a 0.1 M concentration and $\Delta pH = pH - pH_{zpc}$ of -1.35 units. This comparison may indicate that the results obtained with the acid-base potentiometric titrations overestimate the adsorption capacity of H^+ and OH^- ions of the α-Cr_2O_3 samples and, therefore, the σ_0 data in Fig. 7 are not indicative of the true surface charge of the oxide.

These "unrealistic" values of surface charge may explain the high capacity values obtained by fitting the curves with a triple layer model (Fig. 7). Therefore, another interpretation is that, in addition to the H^+ and/or OH^- ions consumed by the oxide surface in order to develop charge, other reactions which consume these ions during the potentiometric titrations must also be occurring simultaneously.

A spectrophotometric analysis of the supernatant obtained after performing some titrations on the oxide suspensions revealed the presence of soluble Cr(VI) species. For the oxide sample obtained at 400° C around 5×10^{-5} mol of soluble Cr(VI) species per gram of titrated sample was observed in the supernatant. A similar fact was observed by Yates and Healy [24]. These authors found that even after exhaustive washing of the samples, the Cr(VI) species on the solid material were not thoroughly removed and these species were always found dissolved in the solution in contact with oxide particles. In the present work this fact was corroborated.

These results suggest that during the calcination stage a small amount of Cr(III) hydroxide decomposes to Cr(VI) oxide, possibly according to the following expression:

$$2Cr(OH)_3(s) + 6O_2 \xrightarrow{T > 400° C} 2CrO_3(s) + 3H_2O \qquad (9)$$

and is then dissolved according to

$$CrO_3(s) + H_2O \longrightarrow H_2CrO_4(aq)$$
$$\rightleftharpoons HCrO_4^-(aq) + H^+ \qquad (10)$$

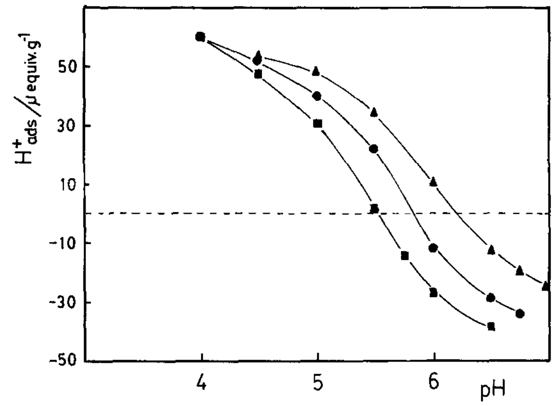

Fig. 8. Potentiometric titration curves corresponding to Fig. 7, corrected taking into account the formation of Cr(VI) species in the solid particle and its chemical equilibrium in solution. $NaNO_3$: (■) 0.5, (●) 0.1 and (▲) 0.01 N.

From the electrophoretic study of $Cr(OH)_3$ samples calcined at different temperatures up to 1200° C, Bye and Simpkin [25] observed the formation of Cr(VI) species during calcination and also during the ageing of the oxide in aqueous solution. These authors concluded that some of these Cr(VI) compounds remain in the surface of the Cr_2O_3, modifying considerably the acid-base behaviour of the Cr_2O_3-aqueous solution interface. This fact has not been proved so far in our laboratories though some work with this aim is in progress.

On the other hand, the acid-base properties of the Cr(VI) species in solution can also markedly affect the shape of the titration curves. The inflection point observed at pH values between 7.5 and 8.0 can be explained for the equilibrium

$$HCrO_4^- \rightleftharpoons CrO_4^{2-} + H^+ \qquad (11)$$

which has a minimum buffer capacity in this pH range.

Taking into account the presence of Cr(VI) species in solution, it can be concluded that the $(\Gamma_{H^+} - \Gamma_{OH^-})$ values shown in Fig. 7 correspond to the H^+ or OH^- ions adsorbed by the oxide to develop surface charge plus those consumed by the soluble Cr(VI) species through the equilibria of Equations 10 and 11. Thus, to find the true adsorption capacity of H^+ and/or OH^- ions by the oxide particle surface it is necessary to make corrections on the potentiometric titration data.

From the amount of Cr(VI) formed and dissolved in aqueous solution per gram of sample and knowing the acid equilibrium constant values of H_2CrO_4, it is possible to correct the experimental titration curves. The corrected curves expressed as microequivalents of H^+ ions adsorbed per gram of sample as a function of pH are shown in Fig. 8, where the negative values stand for the adsorption of hydroxyl ions.

Regazzoni [1] reported that the titration curves for hematite in the presence of phosphate ions in solution show an increment in H^+ ion adsorption due to the adsorption of phosphate ions, which give rise to a displacement of the titration curve to higher pH. On the other hand, Davis and Leckie [26] showed that both $HCrO_4^-$ and CrO_4^{2-} ions adsorb on hydrous iron oxides. Thus, it is possible that the displacement of the titration curves to higher pH values (Fig. 8) is due to the adsorption of aqueous Cr(VI) species on the Cr_2O_3 particle.

As the Cr(VI) species are not completely removed from the solid even after exhaustive washing of the samples and not knowing their effect on the electrophoretic mobilities of the α-Cr_2O_3, the IEP and the CIP obtained from the studied samples cannot be considered as the IEP and the ZPC of pure α-Cr_2O_3. Adsorption studies of $HCrO_4^-$ and CrO_4^{2-} ions on α-Cr_2O_3, which are in progress in our laboratory, may contribute an insight into the behaviour of the aqueous oxide/solution interface of the samples obtained from thermal treatments on chromium(III) hydroxide precursors.

4. Conclusions

The complex *i–E* response observed with Ti/TiO_2-Cr_2O_3 electrodes obtained from calcination of thin coatings of $Cr(OH)_3$ on metallic titanium can be attributed to the presence of chromium oxide species in oxidation state (III) and higher. The maximum current distribution between the different anodic processes is modified according to the temperature and time employed in the calcination step. The process with lower peak potential is predominant at higher temperature and over a long time.

The presence of Cr(VI) species produced during the thermal treatment was observed from chemical analyses performed on the supernatant obtained by washing the powder samples of calcined chromium(III) hydroxide.

The surface acid-base characteristics of colloidal suspensions of chromium(III) oxide samples obtained by potentiometric acid-base titrations and electrophoretic mobility techniques not only correspond to a surface process of adsorption/desorption of H^+ (or OH^-) ions but implies, to a variable degree, some acid-base equilibria in bulk solution due to the presence of chromium species with oxidation states higher than (III).

The different behaviour observed between the variation of the anodic peak potentials in the voltamperograms and the rest potential values of the Ti/TiO_2-Cr_2O_3 electrodes with change in pH suggests that the zone where the electron transfer process occurs in the oxidation of Cr(III) (or from other oxidation state) to Cr(VI) is located in an inner layer of the surface film, very probably situated in the mixed oxide [TiO_2-Cr_2O_3] region formed from the thermal oxidation of the substrate and the incorporation of the chromium(III) oxide produced from the dehydration of the deposited chromium(III) hydroxide.

Acknowledgements

The authors wish to thank the Consejo Nacional de Investigaciones Científicas y Técnicas de Argentina (CONICET) and the Consejo de Investigaciones de la Provincia de Córdoba (CONICOR) for partial financial support. M. J. A. thanks CONICOR for a fellowship. Thanks are also expressed to Mr. Lavilla (CNEA, Córdoba, Argentina) and Dr A. Regazzoni (CNEA, Buenos Aires, Argentina) for their cooperation in the experimental section; to Miss L. P. Falcón for editorial work and language assistance and Dr G. Darbyshire for helpful comments.

References

[1] A. E. Regazzoni, Ph. D. Thesis, Universidad Nacional de Tucuman, Argentina (1984).
[2] F. Beck and H. Schulz, *Ber. Bunsenges Phys. Chem.* **88** (1984) 155.
[3] *Idem*, *Electrochim. Acta* **29** (1984) 1569.
[4] *Idem*, *J. Electroanal. Chem.* **229** (1987) 339.
[5] *Idem*, *J. Appl. Electrochem.* **17** (1987) 739.
[6] O. R. Cámara, XVIII Congreso Latinoamericano de Química, Santiago de Chile (January 1988).
[7] O. R. Cámara and C. P. De Pauli, VIII Reunión Latinoamericana de Electroquímica y Corrosión, Huerta Grande, Córdoba, Argentina (November 1988).
[8] O. R. Cámara, *J. Electroanal. Chem.* **284** (1990) 155.
[9] M. J. Avena, O. R. Cámara and C. P. De Pauli, VII Congreso Argentino de Fisicoquímica, Termas de Río Hondo, Santiago del Estero, Argentina (April 1989).
[10] P. Hesleitner, D. Babic, N. Kallay and E. Matijevic, *Langmuir* **3** (1987) 815.
[11] D. E. Yates, S. Levine and T. W. Healy, *J. Chem. Soc. Faraday Trans. 1* **70** (1974) 1807.
[12] L. Block and P. L. De Bruyn, *J. Colloid. Interf. Sci.* **32** (1970) 518.
[13] D. M. Furlong, D. E. Yates and T. W. Healy, *in* 'Studies in physical and theoretical chemistry' (edited by S. Trasatti), part 11B Electrodes of Semiconductive Metallic Oxides, Ch. 8, Elsevier Scientific (1981).
[14] J. Lyklema, *J. Colloid Interface Sci.* **99** (1984) 109.
[15] To be published.
[16] W. Hill and G. Ohlmann, *J. Catal.* **123** (1990) 147.
[17] M. Pourbaix, 'Atlas of Electrochemical Equilibria in Aqueous Solutions', Pergamon Press, Elmsford, NY (1966).
[18] K. Niki, *in* 'Standard potentials in aqueous solutions: Chromium' (edited by A. J. Bard, R. Pearsons and J. Jordan), Marcel Dekker, New York (1985).
[19] S. Ardizzone and M. Radaelli, *J. Electroanal. Chem.* **269** (1989) 461.
[20] P. Wu, R. Kershaw, K. Dwight and A. Wold, *J. Mat. Sci. Lett.* **6** (1983) 753.
[21] J. A. Kern, H. G. Schwahn and B. Schramm, *Mater. Chem. Phys.* **21** (1989) 391.
[22] R. O. James and G. A. Parks, *in* 'Surface and colloid science', Vol. 12, Plenum Press, New York (1982), Ch. 2.
[23] L. G. J. Fokkink, A. de Keizer and J. Lyklema, *J. Colloid Interface Sci.* **127** (1989) 116.
[24] D. E. Yates and T. W. Healy, *ibid.* **52** (1975) 222.
[25] G. C. Bye and G. T. Simpkin, *Chem. & Ind.* (1970) 532.
[26] J. A. Davis and J. O. Leckie, *J. Colloid Interface Sci.* **74** (1982) 32.